2013

Accuracy of Limited Field Cone Beam Computed Tomography in the Detection of Buccal Cortical Plate Perforations Due to Periapical Lesions

Dan-Linh Ha
Virginia Commonwealth University

Accuracy of Limited Field Cone Beam Computed Tomography in the Detection of Buccal Cortical Plate Perforations Due to Periapical Lesions

A thesis submitted in partial fulfillment of the requirements for the degree of Master of Science in Dentistry at Virginia Commonwealth University.

by

Dan-Linh Ha,
BSc, University of British Columbia, 2005
DDS, Indiana University School of Dentistry, 2010

Director: Karan J. Replogle, DDS, MS,
Program Director, Department of Endodontics,
Virginia Commonwealth University School of Dentistry

Virginia Commonwealth University
Richmond, Virginia
May, 2013

Acknowledgment

The author wishes to thank several people. I would like to thank my family and friends for all of their love and support during the past seven years away from home. I would also like to thank Drs. Replogle, Rathore, Archer and Best for their help and direction with this project. Lastly, I would like to thank my co-residents and Kristin Edwards for their assistance.

Table of Contents

List of Tables

Table

List of Figures

Figure

Abstract

ACCURACY OF LIMITED FIELD CONE BEAM COMPUTED TOMOGRAPHY IN THE DETECTION OF BUCCAL CORTICAL PLATE PERFORATIONS DUE TO PERIAPICAL LESIONS

By Dan-Linh Ha, DDS

A thesis submitted in partial fulfillment of the requirements for the degree of Master of Science in Dentistry at Virginia Commonwealth University.

Virginia Commonwealth University, 2013.

Director: Karan J. Replogle, DDS, MS
Program Director, Department of Endodontics

Pre-surgical planning for endodontic microsurgery is facilitated by the use of cone beam computed tomography (CBCT). The purpose of this study was to determine whether limited field CBCT accurately predicts buccal cortical plate perforations due to endodontic lesions. Thirty-five roots that underwent microsurgical root end resection were included in this study. Prior to the surgery, 90 voxel CBCTs were taken with a Carestream 9300. The scans were analyzed by an endodontic resident and oral radiologist to determine the presence of a perforation in the buccal plate. These findings were compared to the clinical appearance of the bone. There was a significant relationship between a judgment of perforation made on the basis of CBCT and actual perforation as observed clinically. The CBCT prediction was accurate 83% of the time. A predicted perforation was validated in 88% of the instances and a predicted non-perforation was validated in 75% of the instances.

Introduction

Apical periodontitis is inflammation of the periodontium resulting from infection of the tissues of the root canal system and surrounding dentin (1, 2). This can involve progressive stages of inflammation and changes in periapical bone structure, which may be identified as a radiographic radiolucency (3). Radiographs have for years been used as a tool for dental imaging in the detection of apical lesions. They are essential in the diagnosis of apical periodontitis and treatment planning in endodontics.

Controversy exists regarding whether cortical plate involvement is a prerequisite for the radiographic detectability of periapical lesions. Shoha and colleagues (4) created artificial periapical lesions below premolars and second molars in a human cadaver mandible. They demonstrated that lesions confined to cancellous bone in the premolar area could be detected radiographically. In a similar study, Lee and Messer (5) detected lesions limited to cancellous bone in 80% of molar roots. They further reported cortical involvement to enhance visualization. In an animal study correlating the histological and radiographic appearance of induced periapical lesions in dogs, Pitt Ford (6) also concluded that cortical involvement was not necessary for radiographic determination of lesions.

Bender and Seltzer (7, 8) created artificial periapical lesions in mandibles of human cadavers with dental burs and files and radiographed them. They found that lesions in cortical bone could only be detected radiographically when there was a perforation of the bone cortex, erosion from the inner surface of the bone cortex or extensive erosion or destruction from the

outer surface. They concluded that early stages of bone disease cannot be detected on radiographs, nor can the size of a rarefied area on an x-ray be correlated with the amount of tissue destruction. Using cadaver mandibles, Bender (9) deduced that at least 12.5% cortical bone loss with 7.1% mineralized bone loss is required to radiographically visualize apical periodontitis. Width of buccal bone varies with anatomical region, and for this reason, lesion location influences radiographic visualization (2).

Radiographs are two-dimensional images of three-dimensional objects, thus obtaining a complete understanding of the anatomy of these lesions is a challenge. Improved perception of depth and spatial relationship of periapical lesions may be achieved by taking multiple parallax radiographs (10, 11). By comparing radiographic findings with histological analyses, Brynolf (10) found that it was possible to obtain a correct diagnosis from a single radiograph in 74% of cases and in 90% by using three radiographs. Although this technique is widely used in endodontics and aids in making a clinical diagnosis, the buccal-lingual dimension cannot be fully appreciated. Further, geometric distortion of the teeth and overlying dentoalveolar structures in conventional radiographic methods make interpretation of radiographs more difficult (11).

The use of digital radiography in dentistry was first introduced as Radiovisiography by Dr. Francis Mouyen in France in 1987 and was approved by the FDA in 1989 (12, 13). Advantages of its use include instantaneous generation of high-resolution digital images, processing of the image for enhanced diagnostic performance, decrease in radiation dose, ease of archiving and transmission, and reduction in time between exposure and image interpretation (13).

There does not appear to be a consensus in the literature regarding whether digital or conventional radiography is superior in the detection of bur-induced artificial periapical bone

lesions in cadaver jaws (12, 14-17). Mistak and colleagues (12) did not find a significant difference in the detection of lesions between stored direct digital radiographs, telephonically transmitted digital radiographs and conventional D speed film. Paurazas (14) failed to show a difference in lesion detection when comparing E speed film, charged couple device (CCD) sensors and complimentary metal-oxide semiconductor active pixel sensors. The study did conclude that lesions involving the cortical bone were identified with greater accuracy regardless of the imaging system used. E speed film displayed the highest sensitivity and specificity followed by photostimulable phosphor (PSP) plates and CCDs (15). Observers with experience in digital image viewing performed better than those without experience (15). When comparing CCDs to E speed film, Yokota et al (16) found that conventional radiographs were more diagnostic than digital radiographs in the absence of a lesion. When the lesions were enlarged to involve the lamina dura and medullary bone, the CCDs were found to be superior; although there was no difference between the two when the lesion involved the cortical bone (16). In contrast, Hadley et al (17) concluded that filtered direct digital sensors and PSP plates were superior to D speed film in lesion detection.

Cone beam computed tomography (CBCT) has been widely accepted in recent years in dentistry as an adjunct to radiographs in visualizing the endodontic lesion (18). In 2001, The Food and Drug Administration approved the first CBCT unit for dental use in the United States (19). CBCT is an extra-oral imaging system that produces three-dimensional scans of the maxillo-facial skeleton. The X-ray source and detector rotate between 180 and 360 degrees around the patient's head while the patient is either sitting or standing (18). The cone shaped beam captures a cylindrical or spherical volume of data, which is termed the 'field of view.' This

allows for views in the axial, coronal and sagittal planes as well as a 3 dimensional reconstruction.

Decreasing radiation exposure may be accomplished by decreasing the field size and therefore, limiting the field of view (20). Various size CBCT scans are available, 5 cm x 5 cm, 10 cm x 5 cm, 8 cm x 8 cm, 10 cm x 10 cm, 17 cm x 6 cm, 17 cm x 11 cm, and 17 cm x 13.5 cm which allow capture of an image based on disease presentation and region of interest. In general, the smaller the scan volume, the higher the resolution of the image and the lower the effective radiation dose to the patient (21, 22). As the earliest sign of a periapical radiographic finding suggestive of pathosis is discontinuity of the lamina dura and widening of the periodontal ligament space, it is desirable that the optimal resolution of any CBCT imaging system used in endodontics not exceed 200 μm, the average width of the periodontal ligament space (19, 23). For most endodontic applications, limited or focused view CBCT is preferred to improve diagnostic accuracy, decrease radiation exposure to the patient, save time due to smaller volume to be interpreted, decrease field of responsibility and focus on anatomical areas of interest (24).

With CBCT data, the voxels are equal in length, height and depth, which allows for geometrically accurate measurements in any plane (24, 25). Typically, the smaller the field of view for a given system, the lower the radiation dose (20, 21). For the Kodak 9000 3D CBCT focused field, the effective dose is 5.3μSv and 9.8μSv for maxillary anterior and posterior teeth, respectively, and 21.7μSv and 38.3μSv for mandibular anterior and posterior teeth, respectively (26). For comparison, the effective dose of one digital periapical radiograph is 6 μSv. It is needless to say that CBCTs should be reserved for select cases where conventional radiography is inadequate alone. The As Low As Reasonably Achievable or ALARA principle should be considered at all times.

There has been much research suggesting that apical pathology is more easily and accurately detected in CBCT images compared to traditional and digital periapical radiographs (22, 27-32). By creating artificial apical lesions in human cadaver mandibles, Patel et al (22) found digital periapical radiographs and CBCT to have an overall sensitivity of 24.8% and 100%, respectively. Ozen (31) and Sogur (32) also found CBCT images to be superior to both digital and conventional radiography in the detection of chemically created periapical lesions in cadaver mandibles. In a 6-month outcome study on dogs, conventional radiography was unreliable in diagnosing the absence of a lesion and reduction in lesion size compared to CBCT (28). A favorable outcome was determined in 79% of roots using periapical radiographs and in 35% of roots using CBCT, suggesting a higher sensitivity for CBCT (28). In a chart review of 888 patients and 1508 teeth, Estrela et al (27) compared conventional periapical and panoramic films and CBCT in detecting apical periodontitis. The prevalence of apical periodontitis was significantly greater with CBCT.

Recent prospective human studies have shown CBCT to be superior to periapical radiographs in the detection of apical pathology (33-36). Increased numbers of periapical lesions have been detected using CBCT compared to conventional and digital radiographs (33, 34). In the first of a two-part study, Patel et al (35) compared the prevalence of periapical lesions of roots using radiographs and CBCT of teeth treatment planned for endodontic therapy. Periapical lesions were determined in 20% of roots in radiographs and in 48% in CBCT. The subsequent study evaluated the change in lesion size using both imaging modalities one year after nonsurgical root canal therapy (36). The authors found a significant difference in outcome diagnosis between systems. Digital radiography established a healed and healing rate of 92.7% and 97.2%, respectively, which decreased to 73.9% and 89.4% with CBCT (36). CBCT imaging

appears to have greater sensitivity than radiographs, resulting in a difference in NSRCT outcome.

Lofthag-Hansen and colleagues (29) found additional information visible in CBCT images compared to periapical film in a retrospective chart review. They advocated the use of CBCT as they found better visualization of the anatomy of the roots and canals, lesion location and proximity to the maxillary sinus and better understanding of lesion size. They further found erosions or perforations of the buccal and or palatal/lingual plates at the level of the apices were detected 9 times more often in CBCT than in conventional radiographs (29). Low et al (30) compared conventional film to limited field CBCT scans taken of posterior maxillary teeth referred for apical surgery in 53 patients. They found that 34% more lesions were detected by CBCT than in radiographs. Expansion of lesions into the sinus, sinus membrane thickening and missed canals are additional information obtained from the CBCT.

Pinsky et al (37) measured the accuracy of linear and volumetric measurements of artificially created defects with CBCT. Using an acrylic block and cadaver mandible with CBCT voxel size of 0.2 mm, they found a mean width linear accuracy of 0.01 mm for acrylic and 0.07 mm in the mandible. Volume accuracy was 6.9mm for automated calculations and 2.3mm for manual measurements. The authors concluded that such accuracy cannot be repeated on patients because of factors such as differences in bony trabeculation, the presence of soft tissues and patient movement (37).

CBCT allows for an improved understanding of the extent of the lesion and maxillofacial anatomy in three dimensions. Leung et al (38) found that alveolar bone height can be measured to an accuracy of about 0.6mm, and root fenestrations can be identified with greater accuracy than dehiscences with CBCT. Patcas et al (39) compared different CBCT voxel resolutions of

0.125mm and 0.4mm when measuring the bony covering of the mandibular anterior teeth of human cadavers. They concluded that CBCT renders anatomic measurements reliably although the presence of soft tissue and voxel size both affect precision of the data. They could not depict the buccal alveolar bone reliably and there was an overestimation of fenestrations and dehiscences (39). Timock et al (40) used a voxel size of 0.3mm to measure lesions in cadaver mandibles. They found high precision and accuracy when measuring buccal bone height and thickness although buccal bone height had greater reliability and agreement with direct measurements than did the buccal bone thickness measurements.

The current literature suggests a 72-76% healed rate with 84-94% of teeth remaining asymptomatic and functional 4-10 years after root end resection and filling (41-43). The size of the apical periodontal lesion and intraoperative surgical crypt are important prognostic factors for apical surgery. A lesion size less than 5 mm and crypt size less than 10 mm are most favorable (41, 44-46). In teeth with large lesions and crypts, expansion of the crypt is not performed and healing might be compromised by absence of an excisional wound or incomplete curettage of the pathological lesion which may remain as a nidus for persistent infection (45).

Of importance when planning for apical root end resection is the condition of the buccal cortical plate overlying the apical lesion. When the buccal bone is absent, the mucoperiosteal flap may attach to the root surface via long junctional epithelium which may break down at a later time or the epithelium may migrate down the root surface in the early stages of healing and result in a periodontal pocket, allowing reinfection of the endodontic lesion (47). Removal of large portions of facial bone was found to lead to incomplete healing in dogs (48, 49). In a retrospective study of 572 teeth treated with periapical surgery, important factors with significantly improved healing included the presence of bone covering the periapical rarefaction

and the presence of marginal buccal bone (44). In another retrospective study of 27 teeth with complete loss of buccal bone at the time of surgery, only 37% healed after root end resection (47). In a recent randomized controlled study evaluating mineral trioxide aggregate as a retrofill material, periapical bone healing was significantly better for teeth with intact buccal bone than for teeth with a preoperative buccal fenestration due to apical periodontitis (50).

Discrepancies have been noted on numerous occasions in the graduate endodontic clinic at Virginia Commonwealth University, between the findings on the CBCT and clinical presentation of the buccal plate during apical surgery. Specifically, when looking at the CBCT, one may predict that there is a perforation in the buccal cortical plate; however, after reflecting a full thickness mucoperiosteal flap, the cortical plate is, in fact, intact. The purpose of this study was to determine whether limited field CBCT imaging accurately predicts buccal cortical plate perforations due to endodontic lesions.

Materials and Methods

The Virginia Commonwealth University Institutional Review Board approved this study. Electronic chart records of all patients who had microsurgical root end resection completed in the graduate endodontic clinic at Virginia Commonwealth University between July 1, 2011 and August 15, 2012 were reviewed and included in this study. This consisted of CBCT scans, surgical clinical notes, and intraoperative photos from 25 patients. All teeth had previously been endodontically treated at various times, some of which had been nonsurgically retreated. All teeth displayed a failing root canal treatment based on clinical or radiographic findings. 35 roots of 26 teeth (10 anterior teeth and buccal roots of 8 premolar and 8 molar teeth) were evaluated in this study.

The CBCT scans were taken prior to surgery with the Carestream 9300 system (Carestream Health; Rochester, NY). All CBCT images were taken by using a limited field of view (5 x 5 cm) and a voxel size of 0.090 mm. Operating parameters were set at 2-10 mA, 60-90 kV, and 12 seconds.

An endodontic resident and oral and maxillofacial radiologist evaluated the CBCT images. For calibration, the viewers analyzed CBCTs and recorded lesion size and presence of perforation of buccal cortical plate for multiple scans together, and then independently until they came to consensus. The CBCTs in the study were reviewed blinded and independently in four sessions on the same computer under the same lighting and viewing conditions. The CBCTs were examined in all three planes, axial, coronal and sagittal, to determine whether a perforation

in the buccal cortical plate was apparent. Measurements of the lesion were also recorded in all three views. To evaluate intra-rater reliability, each observer repeated the evaluation of five scans during one session at a later date. CBCT images were analyzed by using a Dell Optiplex 990 computer (Dell SA, Geneva, Switzerland) and a 22-inch LCD monitor with a resolution of 1680 x 1050 pixels (Dell SA, Geneva, Switzerland).

Patient charts were reviewed by the primary author after completion of the CBCT analysis. From the patients' dental chart note, the surgeon's documentation of the presence or absence of a buccal plate perforation was recorded. There were a total of five surgeons who made the clinical determination. The surgeon's documentation was confirmed with available intraoperative photographs. These findings were then compared to the findings from the CBCTs.

Results

Patient demographics and characteristics of the 35 roots evaluated in this study are described in Tables 1 and 2, respectively. There were 10 anterior roots and 25 posterior; and 24 maxillary roots and 11 mandibular. Whether or not a perforation was present in the buccal cortical plate overlying the lesion was assessed at the time of surgery. There were significantly more perforations in the anterior than the posterior regions (90% versus 52%, $P = 0.0244$). There was no significant difference between perforations in the maxilla versus mandible (67% versus 55%, $P > 0.49$).

Table 1: Patient Demographics (N = 25)

Demographics		
Sex		
	Female	10
	Male	15
Race/Ethnicity		
	Asian	2
	Black	1
	Hispanic	2
	White	20
Age		
	Mean	56.7
	SD.	17.1
	Min.	16
	Max.	85

Table 2: Root Characteristics and the Number Perforating Buccal Bone (N = 35)

Anteroposterior	Arch	Tooth	Yes	No	total
Anterior	Maxillary	6	1	0	1
		7	1	1	2
		8	2	0	2
		9	2	0	2
	Mandibular	24	1	0	1
		25	2	0	2
		total	9	1	10
Posterior	Maxillary	3	0	2	2
		4	1	1	2
		5	1	0	1
		12	4	0	4
		14	4	4	8
	Mandibular	19	1	3	4
		21	1	1	2
		30	1	1	2
		total	13	12	25

Whereas Table 2 shows the location and number of teeth actually perforated, a predicted perforation was diagnosed from the CBCT by two raters independently. When one viewer predicted perforation, the other agreed with the diagnosis 88.6% of the time (Kappa = 76.2%, 95% CI = 54.3 to 98.1).

Figures 1-3 depict sagittal, coronal and axial views of limited field CBCT of upper left maxillary molar tooth #14. Apical pathology appears to be associated with the mesiobuccal root. Discontinuity of the buccal cortical plate is visualized adjacent to the lesions in coronal and axial planes. This finding was in agreement with the clinical representation of buccal bone after reflection of a full thickness mucoperiosteal flap prior to root end resection. As illustrated in Figure 4, there is a distinct break in the buccal bone.

Figure 1: CBCT Sagittal View of #14

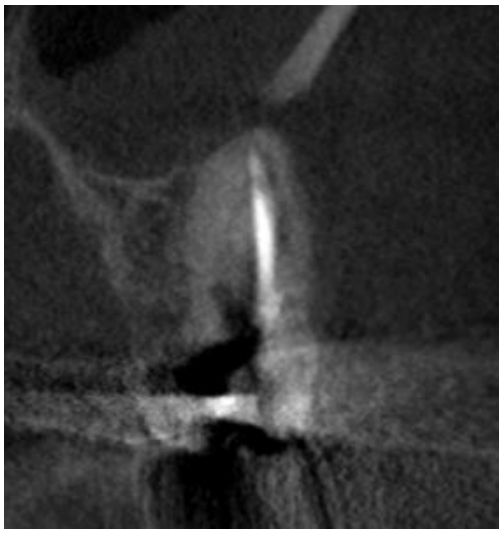

Figure 2: CBCT Coronal View of Mesiobuccal Root of #14

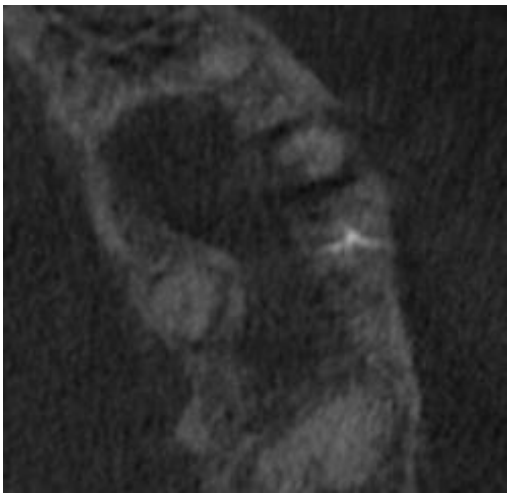

Figure 3: CBCT Axial View of #14

Figure 4: Intraoral Image of #14 After Reflection of Gingival Flap

Figures 5-7 display images of a CBCT scan where both viewers predicted the buccal cortical plate to be intact over the mesial root of #19. This was evidently a false negative as the buccal bone appeared eroded at the time of surgery as illustrated in the clinical photograph in Figure 8.

Figure 5: CBCT Sagittal View of #19

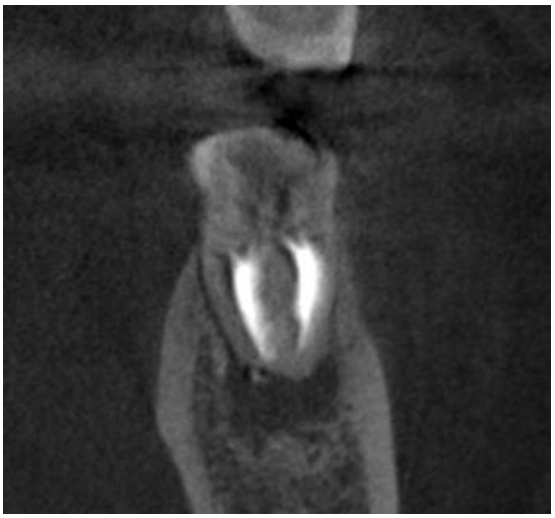

Figure 6: CBCT Coronal View of Mesial Root of #19

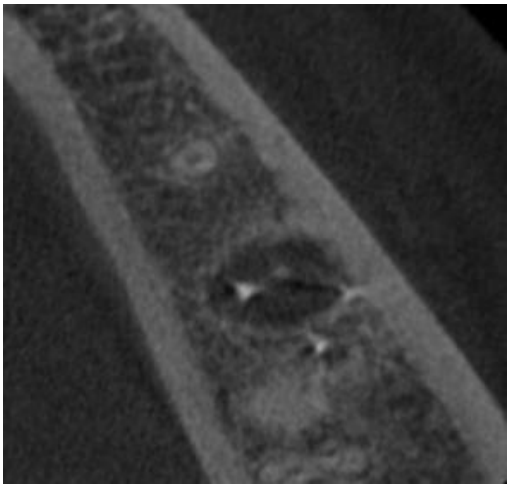

Figure 7: CBCT Axial View of #19

Figure 8: Intraoral Image of #19 After Reflection of Gingival Flap

In the following CBCT represented in Figures 9-11, both viewers predicted a perforation adjacent to the apical lesion. According to the clinical notes and intraoral photos, it appears that a severe periodontal dehiscence was present, however, the bone overlying the periapical lesion was intact.

Figure 9: CBCT Sagittal View of #3

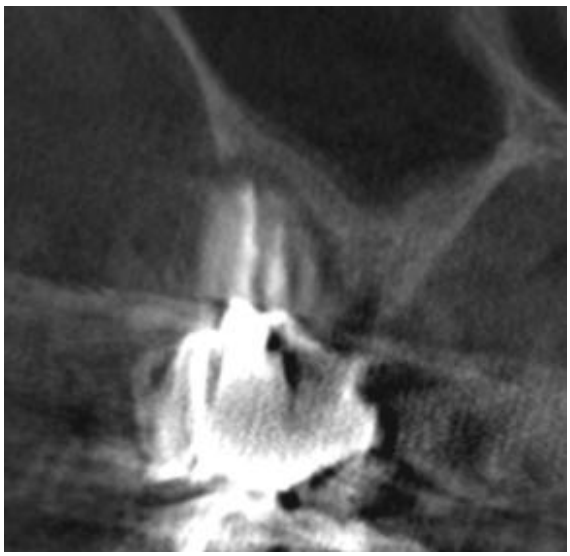

Figure 10: CBCT Coronal View of Mesiobuccal Root of #3

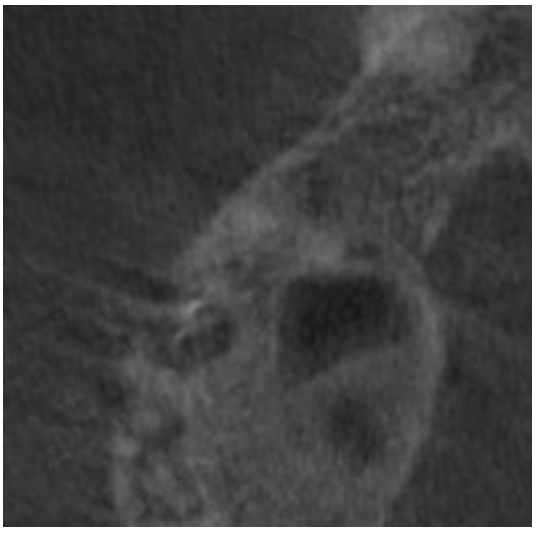

Figure 11: CBCT Axial View of #3

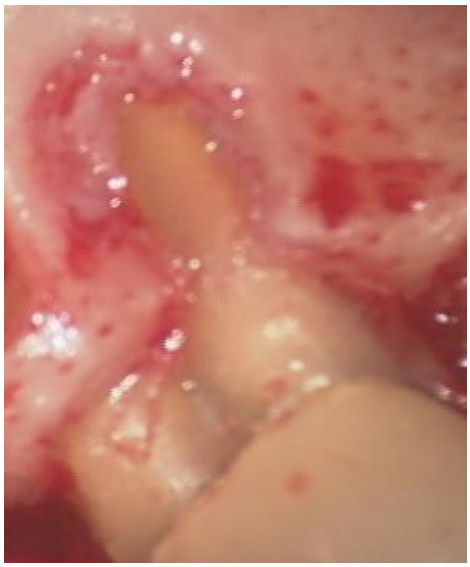

Figure 12: Intraoral Image of #3 After Reflection of Gingival Flap

The primary purpose of the study was to determine the accuracy of a perforation diagnosis based on the CBCT. Using the information from both raters, Table 3 shows that CBCT correctly predicted actual perforation 82.9% of the time. There were 37 true positives and 7 false negatives, giving a sensitivity of 84.1%. There were 21 true negatives and 5 false positives,

giving a specificity of 80.8%. In the 42 instances where CBCT predicted a perforation, the positive predictive value (PPV) was 88.1% and in the 28 instances where CBCT predicted no perforation, the negative predictive value (NPV) was 75.0%. There was a significant relationship between a judgment of perforation made on the basis of CBCT and actual perforation as observed by the surgeon (chi-square=27.8, P < .0001). There was no significant difference between the accuracy of diagnosis given by the two raters (resident accuracy = 85.7% and radiologist accuracy = 80.0%). With the 10 anterior roots, the accuracy was 90.0% and with the 25 posterior roots, the accuracy was 80.0% but this difference was not significant (P > 0.25).

Table 3: Accuracy of CBCT Diagnosis

	Perforation		
CBCT	Yes	No	Total
Yes	37	5	42
No	7	21	28
Total	44	26	70

		95%	CI
Sensitivity=	84.1%	73.3%	94.9%
Specificity=	80.8%	65.6%	95.9%
False Positive=	19.2%	4.1%	34.4%
False Negative=	15.9%	5.1%	26.7%
PPV=	88.1%	78.3%	97.9%
NPV=	75.0%	59.0%	91.0%
Accuracy=	82.9%		
Prevalence=	62.9%		

The secondary aim of the study was to determine if there was a relationship between the size of the lesion evident on the CBCT and whether the overlying buccal bone was perforated. To this end, the length and width of the lesion were measured in all three views. Table 4 shows that in the axial view the average lesion was 5.3mm long and 4.3mm wide, with an average area of 21.9mm^2. The measurements of lesion size were all strongly correlated (r > 0.84).

Table 4: Dimensions of the Lesions (length and width in mm, area in mm^2)

Measurement	Mean	SD	Range	
Axial				
Length	5.26	2.57	1.60	11.90
Width	4.27	2.28	1.40	11.60
Area	21.94	22.93	1.88	108.42
Sagittal				
Length	5.52	2.75	1.50	12.30
Width	4.35	2.42	0.80	11.30
Area	23.60	24.93	0.94	109.16
Coronal				
Length	5.76	2.91	1.70	12.40
Width	4.35	2.35	1.10	11.50
Area	24.39	24.02	1.60	105.68

There is a clear relationship between lesion size and buccal plate perforation. For instance, the correlation between axial length and width is shown in Figure 13. The red colored dots indicate those teeth that were actually perforated and the blue dots indicate those that were actually not perforated. The larger lesions (those in the upper right corner) have more red and the smaller lesions (those in the lower left corner) have more blue. Those with the filled circle were diagnosed using the CBCT image as perforated and those with the empty circle were diagnosed as not perforated. As in Table 3, the 37 instances where CBCT correctly diagnosed a perforation are shown as a filled red circle and the 7 instances where there was a perforation but CBCT incorrectly indicated no perforation are shown as an empty red circle. The 21 instances where CBCT correctly diagnosed no perforation are shown as an empty blue circle and the 5 instances where there actually was no perforation but CBCT incorrectly diagnosed a perforation are shown as a filled blue circle.

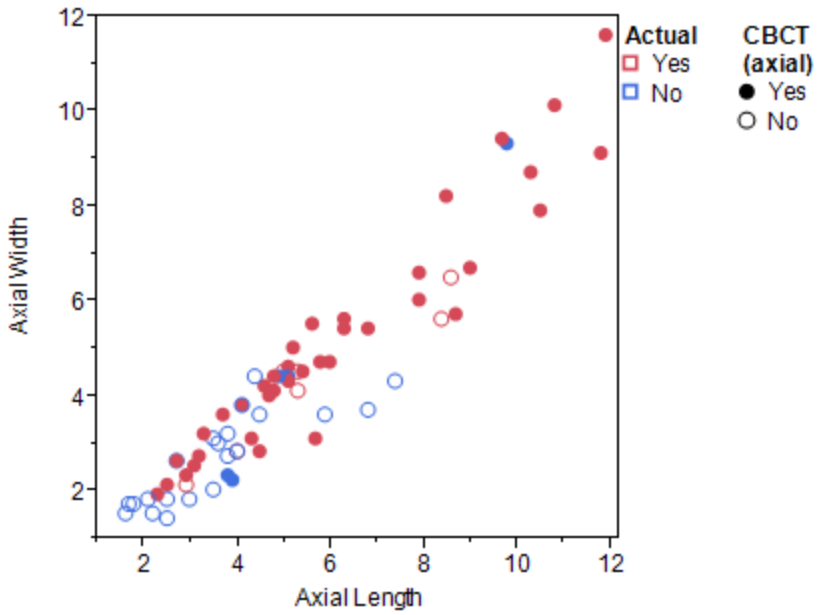

Figure 13: Relationship between Perforation and Lesion Length and Width

A logistic regression model with actual perforation as the outcome and the following predictors: axial length, axial width, posterior, mandibular was run. It indicated that length and width were not significant predictors ($P > 0.18$). A better model uses the area of the lesion, not simply length and width. Specifically, the area of an ellipsoid lesion is $\pi L W/4$, where L is the length and W is the width. A logistic regression model with the following predictors: axial area, posterior, mandibular, and the interaction between axial area and posterior and mandibular was run. It indicated that there was a higher likelihood of perforation in anterior teeth ($P = 0.0487$) and a positive relationship with axial area ($P = 0.0026$). However, although there is no difference between mandibular teeth and maxillary teeth ($P > 0.39$), there is a different relationship with axial area depending upon whether the teeth are mandibular ($P = 0.0809$). The different slope is shown in Figure 14. The predicted probability of Perforation=Yes is shown on the vertical axis and axial area on the horizontal axis. The slope of the curve is much steeper in the mandibular teeth and flatter in the maxillary teeth. Additionally, the anterior teeth (the upper dotted line)

have a higher probability of perforation and the posterior teeth (the lower solid line) have a lower probability of perforation. The horizontal line at 0.7 corresponds to the cutoff that yields the highest sensitivity and specificity. Using this cutoff, the sensitivity is 59.1% and the specificity is 78.4%. That is, a model which uses only tooth location and axial lesion size can significantly predict perforation (chi-square = 21.7, df = 4, P = 0.0002).

Mandibular

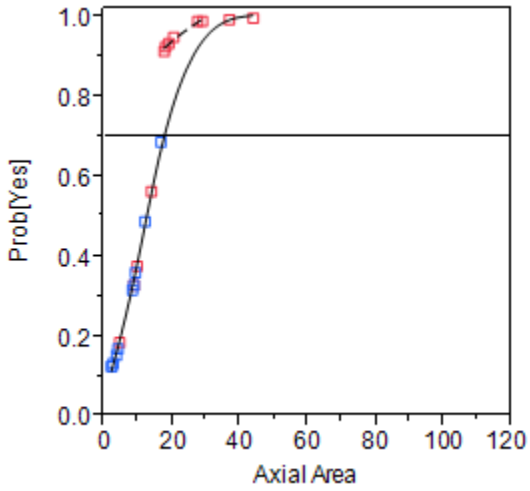

Maxillary

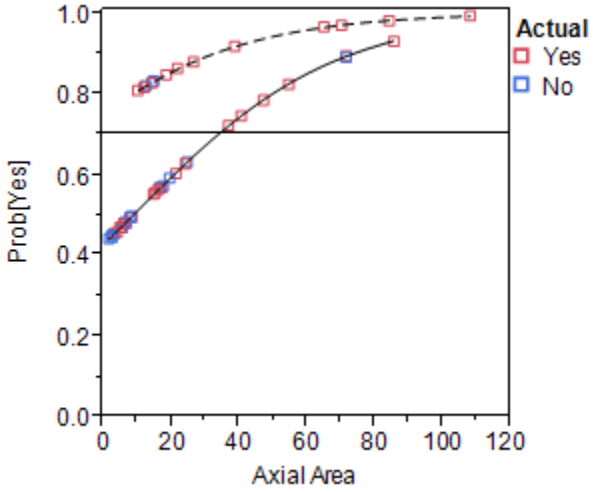

Anterior = upper dotted line; Posterior = lower solid line

Figure 14: Predicted Relationship between Axial Area Depending upon Position

Discussion

In this study, a significant relationship existed between a judgment of perforation made on the basis of CBCT and actual perforation as observed clinically (chi-square=27.8, P <.0001). The CBCT prediction was accurate 82.9% of the time, with sensitivity and specificity of 84.1% and 80.8%, respectively. In this study, sensitivity is defined as the ability to identify perforation of the buccal cortical plate, whereas specificity represents the ability to identify intact buccal bone. A predicted perforation was validated in 88.1% of the instances and a predicted non-perforation was validated in 75.0% of the instances.

Few studies have been published evaluating the width of buccal bone adjacent to roots or endodontic lesions. There has been recent interest in the orthodontic field in determining the presence of naturally occurring bony dehiscences and fenestrations in CBCTs. In a study evaluating the accuracy of CBCT for measuring bony dehiscences and fenestrations of 334 teeth of cadaver skulls, the number of fenestrations detected by CBCT was more than three times higher than for direct examination (38). The sensitivity and specificity were both 81% for fenestrations and 95% and 42% for dehiscences, respectively (38). Although a larger voxel size of 0.38mm was used in the above study, the authors report that the accuracy is not limited by the voxel size, but by the physical spatial resolution of the image. In another human cadaver study, measurements of the bony covering of the mandibular anterior teeth were attempted at 0.125mm and 0.4mm voxel resolutions (39). Voxel size and the presence of soft tissue affected the precision of data and neither resolution depicted the buccal alveolar bone reliably, as there was

an overestimation of fenestrations and dehiscences (39). They concluded that an alveolar thickness of 1 mm might not be accounted for and that there is a risk of assuming the presence of fenestrations from CBCTs that do not exist clinically. In contrast, Timock et al (40) did not find CBCT measurements to differ significantly from direct measurements of buccal alveolar bone height and thickness in cadaver skulls. Although they did not find a pattern of underestimation or overestimation with CBCT measurements, they concluded that buccal bone height had greater reliability and agreement with direct measurements than buccal bone thickness measurements (40). The authors also contributed the discrepancy to poor spatial resolution due to noise and other factors such as beam hardening and scatter.

Evaluating and accurately measuring the thickness of buccal bony plate is a challenging task. Small measurements are especially susceptible to factors affecting accuracy, such as partial volume averaging, noise, and artifacts, making it impossible to achieve a resolution equal to the voxel size (51). Partial volume averaging occurs when the voxel size is larger than the object or the densities it represents. This occurs most often along the margin of an object or at the boundary of the two differing densities. Because the voxel can only display one grey value at a time, the voxel displays an average of the densities to account for this. Partial volume averaging can make boundaries between densities more difficult to accurately distinguish, especially in thin buccal bone, resulting in lower spatial resolution. Spatial resolution refers to the minimum distance needed to distinguish between two objects and is often incorrectly assumed to be equal to a scan's voxel size. Molen (51) recommends using a line pair phantom to determine the unique spatial resolution of the CBCT machine and scan settings used.

One main disadvantage of CBCT is limitation in image quality related to noise and contrast resolution due to scattered radiation (25). CT image artifacts arise from the inherent

polychromatic nature of the projection x-ray beam resulting in beam hardening (25). This leads to distortion of metallic structures due to differential absorption or the presence of streaks and dark bands between two dense objects (25). When evaluating buccal bone thickness, smaller field of views are recommended in order to decrease scatter levels (51). Smaller field of views may decrease noise from scatter but decreasing the voxel size has an inverse effect. As voxels decrease in size, they become more sensitive to noise, resulting in poorer spatial resolution (51). When evaluating CBCTs in this study at 90 voxels, there was some difficulty in determining whether the buccal bone was perforated, as many teeth being evaluated were restored with metallic posts and/or crowns. These restorations lead to the presence of streaks in the surrounding areas. One tooth was adjacent to an implant, which made it difficult to make an accurate determination due to excessive streaking. Patient motion during the scan and the presence of soft tissue are other factors that may have affected the accuracy of measurements.

The secondary aim of the study was to determine if there was a relationship between the size of the lesion evident on the CBCT and buccal bone perforation. The axial area was analyzed as it best represents the relationship between roots and cortical plates of both anterior and posterior teeth. A positive relationship was found between perforation and axial area of endodontic lesion. As the lesion increases in size, there is a larger likelihood of perforating the adjacent bone. When using a logistic regression model, there was a higher likelihood of perforation of buccal bone adjacent to anterior versus posterior teeth (90.0% versus 52.0%).

Although no significant difference existed in number of perforations of buccal bone in maxilla and mandible, a different relationship exists between axial area of lesion and probability of perforation depending on arch type. This is likely due to anatomical differences in alveolar

ridge thickness. A model using only tooth location and axial lesion size may be developed which can significantly predict perforation of the buccal cortical plate.

While a determination of the volume of the lesion would appear to be valuable and might prove to be predictive, the author agrees with Pinsky (37) that the factors such as the differences in bony trabeculations, the presence of soft tissues and patient movement make volume determination, at this time, problematic. Further consideration should be given to the development of CBCT software that can mathematically determine the volume of a lesion. Only then might the volume of a lesion be predictive of a buccal plate perforation.

In the maxilla, the facial cortex is thin in the anterior region and adjacent to the premolars and first molar (2). The buccal cortex of the second and third molar tends to be thicker (2). Eberhardt et al (52) found the buccal bone to be thinnest over the buccal root of the first premolar and thickest over the mesiobuccal root of the second molar. They further determined that an inverse relationship exists between the thickness of bone buccolingually and the bone thickness superior to the apices of the teeth.

In the mandible, the alveolar process is thin in the anterior segment around the incisor roots and becomes thicker in the canine and posterior segments (2). Most root apices of anterior and premolar teeth are located in or near the buccal aspect of the cortical bone (8). In first molars, the mesial root is near the buccal bone plate and the distal root is in cancellous bone or embedded in the lingual bone plate, similar to the apices of second and third molars (2, 8). Bornstein et al (53) measured a mean distance of 5.3 mm from the apices of mandibular molars to the buccal surface of bone, and a buccal cortical bone thickness of 1.7 mm.

Yoshioka et al (54) evaluated and categorized bone defects of 532 endodontically treated teeth with persistent periapical lesions as visualized by CBCT. Lesions were categorized by

anatomical relationship of the bony defect created by the periapical lesion. The percentage of teeth within each category were:

Type I: Cancellous bone defect 22%

Type II: Buccal/labial bone defect 67%

Type III: Palatal/lingual bone defect 4%

Type IV: Through and through bone defect 7%

Type V: Apical root protrusion through bone plate 10%

V-1: Protrusion of apical foramen 4%

V-2: Protrusion of apical one third of root 5%

V-3: Protrusion of whole root 1%

Mandibular teeth had a significantly greater prevalence of type I cancellous bone defects and lower prevalence of type IV through-and-through lesions compared to maxillary teeth. Type II lesions affecting the buccal bone were most common, without significant difference between the maxilla and mandible. Type V lesions, with root apices protruding through the cortical plate, were more prominent in the maxilla (12% versus 2% in the mandible), with the maxillary canine being most affected. The authors attributed the high percentage of buccal bone defects to the natural buccal position of teeth roots.

In this study, the two CBCT raters agreed on the diagnosis of a buccal bone perforation in 88.6% of cases (Kappa 76.2%). There was no significant difference between the two evaluators on any of the measurements of the dimensions of the lesions. When evaluating repeated readings

and lesion measurements, there was less than 0.4% variability due to rater differences and less than 0.2% variability due to repeated measurements done by the same rater.

One challenge when evaluating the buccal bone and measuring lesion size was establishing proper and reproducible alignment of the roots. A small difference in angulation resulted in a significant discrepancy in lesion diameter. Since periapical pathosis is irregular in shape, a small shift in angulation revealed a different dimension. Large lesions that appeared to perforate the buccal cortical plate were difficult to measure, as the original extent of the bone could not be estimated.

There are multiple factors that need to be considered in the present study. This study was a retrospective chart review, and thus, less powerful than a prospective study. There was a time delay between the date that the CBCT scan was taken and the clinical evaluation of buccal cortical plate. In most cases, the scan was taken one to two months prior to endodontic surgery, with a range of 1 to 137 days. This is important to note as during that time frame, the endodontic lesion may have increased in size to involve the bony plate by the time of surgery. In addition, there were five surgeons who independently made the determination of perforation of buccal plate without calibration prior to assessment. This added variability to the study. Furthermore, the study consisted of 35 roots of 26 teeth from all regions of the maxilla and mandible. A larger sample size of each tooth would have been ideal to obtain a more in depth analysis of each tooth type.

Future research should take the above into consideration in addition to the need for endodontic surgery outcome and prospective studies in this area. Outcome studies using CBCT to evaluate healing of the buccal plate and lesion would be beneficial. This type of study would

aid in determining surgical prognostic factors and evaluate the significance of determining the status of the buccal plate preoperatively.

The current literature suggests that CBCT is less accurate in measuring small dimensions such as thickness of buccal plate due to limitations in voxel size and image resolution (38-40). It was determined that as an endodontic lesion increases in size, the probability of perforating the adjacent bone increases in distinct patterns in the maxilla and mandible. In addition, there is a higher likelihood of perforating the buccal bone adjacent to anterior versus posterior teeth. The present study showed that the Carestream 9300 CBCT was accurate 82.9% of the time in predicting buccal cortical plate perforations due to apical periodontitis. While CBCT has proved to be a useful tool for pre-surgical evaluation, the prudent endodontist must be aware of the limitations of CBCT.

References

References

1. Kakehashi S, Stanley HR, Fitzgerald RJ. The effects of surgical exposures of dental pulps in germ-free and conventional laboratory rats. Oral Surg Oral Med Oral Pathol 1965;20:340-9.

2. Huumonen S, Ørstavik D. Radiological aspects of apical periodontitis. Endod Topics 2002;1:3–25.

3. Nair PNR, Sjogren U, Figdor D, Sundqvist G. Persistent periapical radiolucencies of root-filled human teeth, failed endodontic treatments, and periapical scars. Oral Surg Oral Med Oral Pathol Oral Radiol Endod 1999;87:617-27.

4. Shoha RR, Dowson J, Richards AG. Radiographic interpretation of experimentally produced bony lesions. Oral Surg Oral Med Oral Pathol 1974;38:294-303.

5. Lee SJ, Messer HH. Radiographic appearance of artificially prepared periapical lesions confined to cancellous bone. Int Endod J 1986;19:64-72.

6. Pitt Ford TR. The radiographic detection of periapical lesions in dogs. Oral Surg Oral Med Oral Pathol 1984;57:662-7.

7. Bender IB, Seltzer S. Roentgenographic and direct observation of experimental lesions in bone: I. J Am Dent Assoc 1961;62:152-60.

8. Bender IB, Seltzer S. Roentgenographic and direct observation of experimental lesions in bone: II. J Am Dent Assoc 1961;62:708-16.

9. Bender IB. Factors influencing the radiographic appearance of bony lesions. J Endod 1982;8:161-70.

10. Brynolf I. Roentgenologic periapical diagnosis IV. When is one roentgenogram not sufficient? Swed Dent J 1970;63:415-23.

11. Grondahl HG, Huumonen S. Radiographic manifestations of periapical inflammatory lesions. Endod Topics 2004;8:55-67.

12. Mistak EJ, Loushine RJ, Primack PD, West LA, Runyan DA. Interpretation of periapical lesions comparing conventional, direct digital, and telephonically transmitted radiographic images. J Endod 1998;24:262-6.

13. Nair MK, Nair UP. Digital and advanced imaging in endodontics: a review. J Endod 2007;33:1-6.

14. Paurazas SB, Geist JR, Pink FE, Hoen MM, Steiman, HR. Comparison of diagnostic accuracy of digital imaging by using CCD and CMOS-APS sensors with E-speed film in the detection of periapical bony lesions. Oral Surg Oral Med Oral Pathol Oral Radiol Endod 2000;89:356-62.

15. Wallace JA, Nair MK, Colaco MF, Kapa SF. A comparative evaluation of the diagnostic efficacy of film and digital sensors for detection of simulated periapical lesions. Oral Surg Oral Med Oral Pathol Oral Radiol Endod 2001;92:93-7.

16. Yokota ET, Miles DA, Newton CW, Brown CE. Interpretation of periapical lesions using radiovisiography. J Endod 1994;20:490-4.

17. Hadley DL, Replogle KJ, Kirkam JC, Best AM. A comparison of five radiographic systems to D-speed film in the detection of artificial bone lesions. J Endod 2008;34:1111-4.

18. Patel S, Dawood A, Whaites E, Pitt Ford T. New dimensions in endodontic imaging: part 1. Conventional and alternative radiographic systems. Int Endod J 2009;42:447-62.

19. Scarfe WC, Levin MD, Gane D, Farman AG. Use of cone beam computed tomography in endodontics. Int J Dent 2009:1-20.

20. Roberts JA, Drage NA, Davies J, Thomas DW. Effective dose from cone beam CT examinations in dentistry. Brit J Radiol 2009;82:35-40.

21. Ludlow JB, Davies-Ludlow LE, Brooks SL, Howerton WB. Dosimetry of 3 CBCT devices for oral and maxillofacial radiology: CB Mercuray, NewTom 3G and i-CAT. Dentomaxillofac Rad 2006;35:219-26.

22. Patel S, Dawood A, Mannocci F, Wilson R, Pitt Ford T. Detection of periapical bone defects in human jaws using cone beam computed tomography and intraoral radiography. Int Endod J 2009;42:507-15.

23. Kaffe I, Gratt BM. Variations in the radiographic interpretation of the periapical dental region. J Endod 1988;14:330-5.

24. Scarfe WC, Farman AG, Sukovic P. Clinical applications of cone beam computed tomography in dental practice. J Can Dent Assoc 2006;72:75-80.

25. Scarfe WC, Farman AG. What is cone beam CT and how does it work? Dent Clin N Am 2008;52:707-30.

26. Ludlow JB. Dosimetry of the Kodak 9000 3D small FOV CBCT and panoramic unit. Oral Surg Oral Med Oral Pathol Oral Radiol Endod. 2008;107:e29.

27. Estrela C, Bueno MR, Leles CR, Azevedo B, Azevedo JR. Accuracy of cone beam computed tomography and panoramic and periapical radiography for detection of apical periodontitis. J Endod 2008;34:273-9.

28. Garcia de Paula-Silva FW, Hassan B, Bezerra da Silva LA, Leonardo MR, Wu MK. Outcome of root canal treatment in dogs determined by periapical radiography and cone-beam computed tomography scans. J Endod 2009;35:723-6.

29. Lofthag-Hansen S, Huumonen S, Gröndahl K, Gröndahl HG. Limited cone-beam CT and intraoral radiography for the diagnosis of periapical pathology. Oral Surg Oral Med Oral Pathol Oral Radiol Endod. 2007;103:114-9.

30. Low KM, Dula K, Bürgin W, von Arx T. Comparison of periapical radiography and limited cone-beam tomography in posterior maxillary teeth referred for apical surgery. J Endod 2008;34:557-62.

31. Ozen T, Kamburoğlu K, Cebeci AR, Yüksel SP, Paksoy CS. Interpretation of chemically created periapical lesions using 2 different dental cone-beam computerized tomography units, an intraoral digital sensor, and conventional film. Oral Surg Oral Med Oral Pathol Oral Radiol Endod 2009;107:426-32.

32. Sogur E, Baksi BG, Gröndahl HG, Lomcali G, Sen BH. Detectability of chemically induced periapical lesions by limited cone beam computed tomography, intra-oral digital and conventional film radiography. Dentomaxillofac Radiol 2009;38:458-64.

33. Abella F, Patel S, Duran-Sindreu F, Mercade M, Bueno R, Roig M. Evaluating the periapical status of teeth with irreversible pulpitis by using cone-beam computed tomography scanning and periapical radiographs. J Endod 2012;38:1588-91.

34. Cheung GSP, Wei WLL, McGrath C. Agreement between periapical radiographs and cone-beam computed tomography for assessment of periapical status of root filled molar teeth. Int Endod J 2013 Feb 5. doi: 10.1111/iej.12076.

35. Patel S, Wilson R, Dawood A, Mannocci F. The detection of periapical pathosis using periapical radiography and cone beam computed tomography-Part 1: pre-operative status. Int Endod J 2012;45:702-10.

36. Patel S, Wilson R, Dawood A, Foschi F, Mannocci F. The detection of periapical pathosis using digital periapical radiography and cone beam computed tomography-Part 2: a 1-year post-treatment follow-up. Int Endod J 2012;45:711-23.

37. Pinsky HM, Dyda S, Pinsky RW, Misch KA, Sarment DP. Accuracy of three-dimensional measurements using cone-beam CT. Dentomaxilllofac Radiol 2006;35:410-6.

38. Leung CC, Palomo L, Griffith R, Hans MG. Accuracy and reliability of cone-beam computed tomography for measuring alveolar bone height and detecting bony dehiscences and fenestrations. Am J Orthod Dentofacial Orthop 2010;137:S109-19.

39. Patcas R, Müller L, Ullrich O, Peltomäki T. Accuracy of cone-beam computed tomography at different resolutions assessed on the bony covering of the mandibular anterior teeth. Am J Orthod Dentofacial Orthop 2012;141:41-50.

40. Timock AM, Cook V, McDonald T, Leo MC, Crowe J, Benninger BL, Covell DA Jr. Accuracy and reliability of buccal bone height and thickness measurements from cone-beam computed tomography imaging. Am J Orthod Dentofacial Orthop 2011;140:734-44.

41. Barone C, Dao TT, Basrani BB, Wang N, Friedman S. Treatment outcome in endodontics: the Toronto study--phases 3, 4, and 5: apical surgery. J Endod 2010;36:28-35.

42. Torabinejad M, Corr R, Handysides R, Shabahang S. Outcomes of nonsurgical retreatment and endodontic surgery: A systematic review. J Endod 2009;35:930-7.

43. von Arx T, Jensen SS, Hanni S, Friedman S. Five-year longitudinal assessment of the prognosis of apical microsurgery. J Endod 2012;38:570-9.

44. Hirsch JM, Ahlstrom U, Henrikson PA, Heyden G, Peterson LE. Periapical surgery. Int J Oral Surg 1979;8:173-85.

45. Wang N, Knight K, Dao T, Friedman S. Treatment outcome in endodontics-the Toronto study. Phases I and II: apical surgery. J Endod 2004;30:751-61.

46. von Arx T, Peñarrocha M, Jensen S. Prognostic factors in apical surgery with root-end filling: a meta-analysis. J Endod 2010;36:957-73.

47. Skoglund A, Persson G. A follow-up study of apicoectomized teeth with total loss of the buccal bone plate. Oral Surg Oral Med Oral Pathol 1985;59:78-81.

48. Boyne PJ, Lvon HW, Miller CW. The effects of osseous implant materials on regeneration of alveolar cortex. Oral Surg Oral Med and Oral Pathol 1961;14:369-78.

49. Hjorting-Hansen E. Studies on implantation of anorganic bone in cystic jaw lesions. 1970. Munksgaard. Copenhagen, Denmark.

50. Christiansen R, Kirkevang LL, Horsted-Bindslev P, Wenzel A. Randomized clinical trial of root-end resection followed by root-end filling with mineral trioxide aggregate or smoothing of the orthograde gutta-percha root filling – 1-year follow-up. Int Endod J 2009;42:105-14.

51. Molen AD. Considerations in the use of cone-beam computed tomography for buccal bone measurements. Am J Orthod Dentofacial Orthop 2010;137:S130-5.

52. Eberhardt JA, Torabinejad M, Christiansen EL. A computed tomographic study of the distances between the maxillary sinus floor and the apices of the maxillary posterior teeth. Oral Surg Oral Med Oral Pathol 1992;73:345-6.

53. Bornstein MM, Lauber R, Sendi P, von Arx T. Comparison of periapical radiography and limited cone-beam computed tomography in mandibular molars for analysis of anatomical landmarks before apical surgery. J Endod 2011;37:151-7.

54. Yoshioka T, Kikuchi I, Adorno CG, Suda H. Periapical bone defects of root filled teeth with persistent lesions evaluated by cone-beam computed tomography. Int Endod J 2011;44:245-52.

Appendix

CBCT Evaluation Form

Evaluator: _____ **Date: _____**

Patient: _____ **Tooth#/Root: _____**

Is the buccal cortical plate perforated in the following views? If a perforation is present, record the size of the lesion.

	Yes	No	Unable to Determine	Size of Lesion	Slice #
Axial	☐	☐	☐	_____mm x _____mm	_____
Sagittal	☐	☐	☐	_____mm x _____mm	_____
Coronal	☐	☐	☐	_____mm x _____mm	_____

Perforation = an opening/hole in the cortical plate overlying a periapical lesion

9300 Carestream 3D Imaging version 3.1.9 at 90 micrometers

Figure 15: CBCT Evaluation Form

Chart Findings of Clinical Status of Buccal Cortical Plate Form

Resident: _____ **Date of Surgery: _____**

Patient: _____ **Tooth # _____**

Demographic Data

Sex _____

Age _____

Ethnicity _____

	Yes	No
1. Was there a periodontal dehiscence?	☐	☐
2. Was there a periodontal fenestration?	☐	☐
3. Was there a perforation in the buccal cortical plate apart from dehiscence and fenestration?	☐	☐

Size of perforation: _____mm x _____mm

Comments:

Perforation = an opening/hole in the cortical plate overlying a periapical lesion
Dehiscence = the bursting through bone of a root as the tooth erupts so that the bone does not extend to its normal proximity to the CEJ
Fenestration = a circumscribed defect that creates a "window" through the bone over the prominent root

Figure 16: Chart Findings of Clinical Status of Buccal Cortical Plate Form

Predicted perforation was diagnosed by two raters independently, an endodontic resident (DH) and a radiologist (SR). A diagnosis was given from the axial view for all roots. For anterior roots, a diagnosis was given from the sagittal view and for posterior roots, a diagnosis was given from the coronal view. The agreement between the two raters is shown in Table 5. Agreement occurred in 88.6% of the cases and the chance-corrected Kappa was 76.2% (95% CI = 54.3 to 98.1). For the five roots selected for repeat assessment, there was perfect agreement between the two raters. (In the axial view, both raters agreed that 3 out of the 5 were perforated.)

Table 5: Inter-rater Agreement on Perforation Diagnosis from the Axial View

	SR		
DH	Yes	No	Total
Yes	19	2	21
No	2	12	14
Total	21	14	35

The agreement when diagnosing from the sagittal view is shown in Table 6. Agreement = 80.0%; Kappa = 37.5% (95% CI = -32.8 to 100.0). For the buccal plate adjacent to five roots selected for a repeat assessment, only one was judged on the sagittal view as perforated by both raters. Another buccal plate adjacent to a root was rated as not perforated by SR and unknown by DH. Agreement from the coronal view is shown in Table 7. Agreement = 92.0%; Kappa = 84.0% (95% CI = 62.7 to 100.0). In the four roots selected for repeat assessment and rated on the coronal view, both raters agreed that two had perforations of buccal bone and two did not.

Table 6: Inter-rater Agreement on Perforation Diagnosis from the Sagittal View (Anterior Roots)

	SR		
DH	Yes	No	Total
Yes	7	1	8
No	1	1	2
Total	8	2	10

Table 7: Inter-rater Agreement on Perforation Diagnosis from the Coronal View (Posterior Roots)

	SR		
DH	Yes	No	Total
Yes	12	1	13
No	1	11	12
Total	13	12	25

Additionally, with 5 roots evaluated by two raters on repeated occasions, we may estimate the measurement variability of the numeric measurements. Each measurement is summarized in Table 8. If each rater (SR, DH) recorded the same number on both of the repeated measurements then there would be 0% variance associated with rater or repeat in the table below. All of the variance would be due to patient-to-patient variability; that is the percent variance for patient would be near 100%. As may be seen, there is less than 0.4% of all variability due to rater differences and less than 0.2% of all variability due to repeated measurements done by the same rater.

Table 8: Variance Components of Measured Values

	% Variance			
	Rater	Repeat	Patient	Residual
Axial Length	0.11	0.11	98.10	1.70
Axial Width	0.20	0.08	98.60	1.10
Sagittal Length	0.16	0.17	97.60	2.10
Sagittal Width	0.06	0.06	99.10	0.80
Coronal Length	0.07	0.04	99.40	0.51
Coronal Width	0.43	0.07	98.70	0.79
Axial Area	0.30	0.14	97.40	2.20
Sagittal Area	0.11	0.14	98.30	1.40
Coronal Area	0.22	0.08	98.60	1.10

The accuracy of the CBCT diagnosis was assessed separately for the two raters.

Table 9: Accuracy of CBCT Diagnosis by DH

	Perforation		
CBCT	Yes	No	Total
Yes	19	2	21
No	3	11	14
Total	22	13	35

		lower	upper
Sensitivity=	86.4%	72.0%	100.0%
Specificity=	84.6%	65.0%	100.0%
False Positive=	15.4%	0.0%	35.0%
False Negative=	13.6%	0.0%	28.0%
PPV=	90.5%	77.9%	100.0%
NPV=	78.6%	57.1%	100.0%
Accuracy=	85.7%		
Prevalence=	62.9%		

Table 10: Accuracy of CBCT Diagnosis by SR

	Perforation		
CBCT	Yes	No	Total
Yes	18	3	21
No	4	10	14
Total	22	13	35

		lower	upper
Sensitivity=	81.8%	65.7%	97.9%
Specificity=	76.9%	54.0%	99.8%
False Positive=	23.1%	0.2%	46.0%
False Negative=	18.2%	2.1%	34.3%
PPV=	85.7%	70.7%	100.0%
NPV=	71.4%	47.8%	95.1%
Accuracy=	80.0%		
Prevalence=	62.9%		

Separate accuracy was determined for the anterior and posterior roots. Although there was significantly more perforation adjacent to anterior roots (chi-square = 6.1, $P = 0.0137$), there was no significant difference in the accuracy of CBCT prediction in anterior roots (chi-square = 1.3, $P = 0.2539$).

Table 11: Accuracy of CBCT Diagnosis Adjacent to Anterior Roots

	Perforation		
CBCT	+	–	Total
+	16	0	16
–	2	2	4
Total	18	2	20

		lower	upper
Sensitivity=	88.9%	74.4%	100.0%
Specificity=	100.0%	100.0%	100.0%
False Positive=	0.0%	0.0%	0.0%
False Negative=	11.1%	0.0%	25.6%
PPV=	100.0%	100.0%	100.0%
NPV=	50.0%	1.0%	99.0%
Accuracy=	90.0%		
Prevalence=	90.0%		

Table 12: Accuracy of CBCT Diagnosis Adjacent to Posterior Roots

	Perforation		
CBCT	+	–	Total
+	21	5	26
–	5	19	24
Total	26	24	50

		lower	upper
Sensitivity=	80.8%	65.6%	95.9%
Specificity=	79.2%	62.9%	95.4%
False Positive=	20.8%	4.6%	37.1%
False Negative=	19.2%	4.1%	34.4%
PPV=	80.8%	65.6%	95.9%
NPV=	79.2%	62.9%	95.4%
Accuracy=	80.0%		
Prevalence=	52.0%		

The measurements of the dimensions of the lesions are summarized by the two evaluators in Table 13. There was no significant difference between the two evaluators on any of the measurements. As shown in Table 14 and Figure 17, there was a high correlation between all of the length and width measurements ($r > 0.84$).

Table 13: Dimensions of the Lesions (length and width in mm, area in mm^2) by Evaluator

Measurement	Evaluator	Mean	SD	Range	
Axial					
Length	DH	5.27	2.49	1.7	11.9
	SR	5.25	2.68	1.6	11.8
Width	DH	4.27	2.32	1.5	11.6
	SR	4.27	2.27	1.4	10.1
Area	DH	21.80	23.15	2.3	108.4
	SR	22.08	23.05	1.9	85.7
Sagittal					
Length	DH	5.57	2.81	1.5	12.3
	SR	5.47	2.73	1.5	12.3
Width	DH	4.31	2.41	0.8	11.3
	SR	4.39	2.47	1.0	10.2
Area	DH	23.37	25.20	0.9	109.2
	SR	23.84	25.03	1.5	97.7
Coronal					
Length	DH	5.93	3.11	2.2	12.4
	SR	5.58	2.72	1.7	12.4
Width	DH	4.41	2.49	1.2	11.5
	SR	4.29	2.23	1.1	9.9
Area	DH	25.74	25.85	2.1	105.7
	SR	23.05	22.33	1.6	96.4

Table 14: Correlation between the Length and Width Measurements

Correlations

	Axial Length	Axial Width	Sagittal Length	Sagittal Width	Coronal Length	Coronal Width
Axial L.	1.0000	0.9483	0.9163	0.9055	0.8904	0.9053
Axial W.	0.9483	1.0000	0.9244	0.9493	0.8549	0.9146
Sagittal L.	0.9163	0.9244	1.0000	0.9212	0.9200	0.9182
Sagittal W.	0.9055	0.9493	0.9212	1.0000	0.8410	0.9199
Coronal L.	0.8904	0.8549	0.9200	0.8410	1.0000	0.8972
Coronal W.	0.9053	0.9146	0.9182	0.9199	0.8972	1.0000

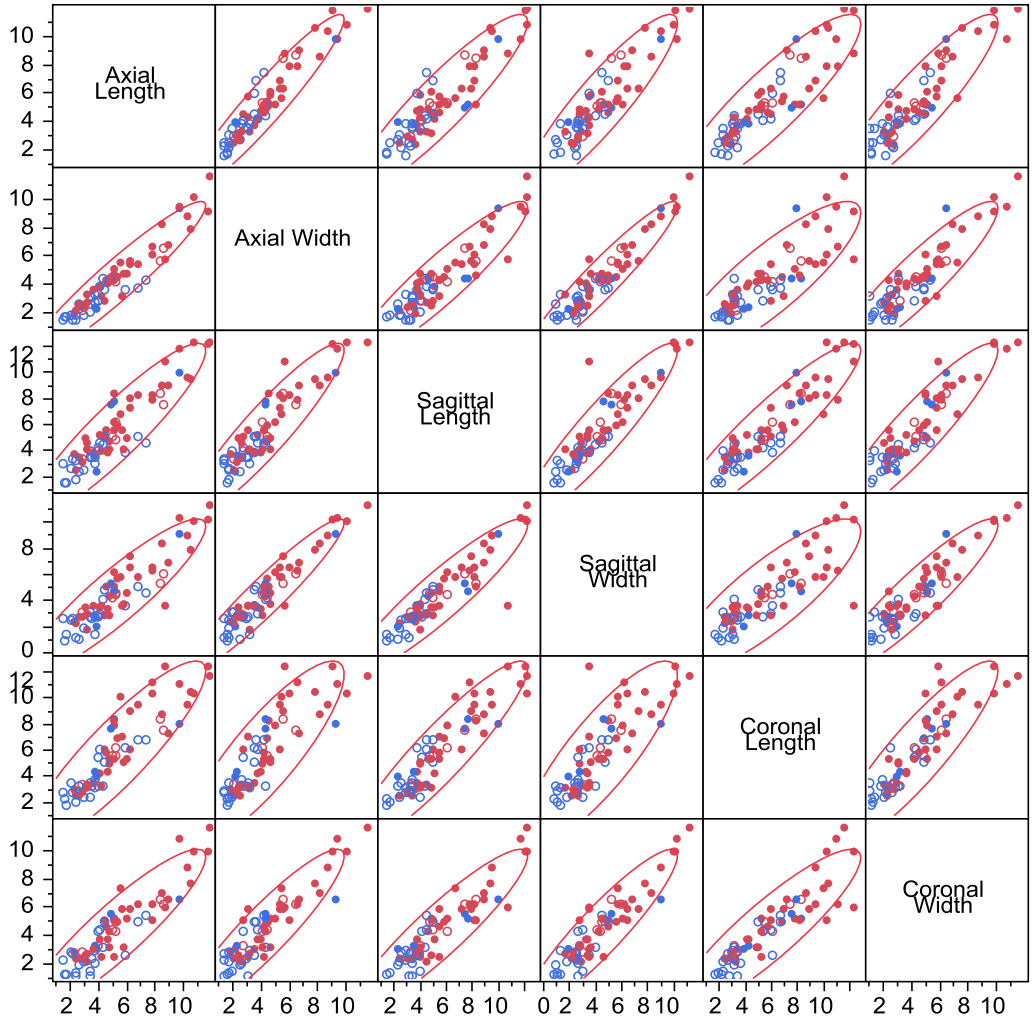

Figure 17: Correlation between the Length and Width Measurements

The area of the lesion, as calculated from all three views, were also highly correlated ($r > 0.93$).

The two raters' measurements were also highly correlated ($r > 0.78$).

Table 15: Correlation between the Areas

	Axial Area	Sagittal Area	Coronal Area
Axial Area	1.0000	0.9681	0.9258
Sagittal Area	0.9681	1.0000	0.9425
Coronal Area	0.9258	0.9425	1.0000

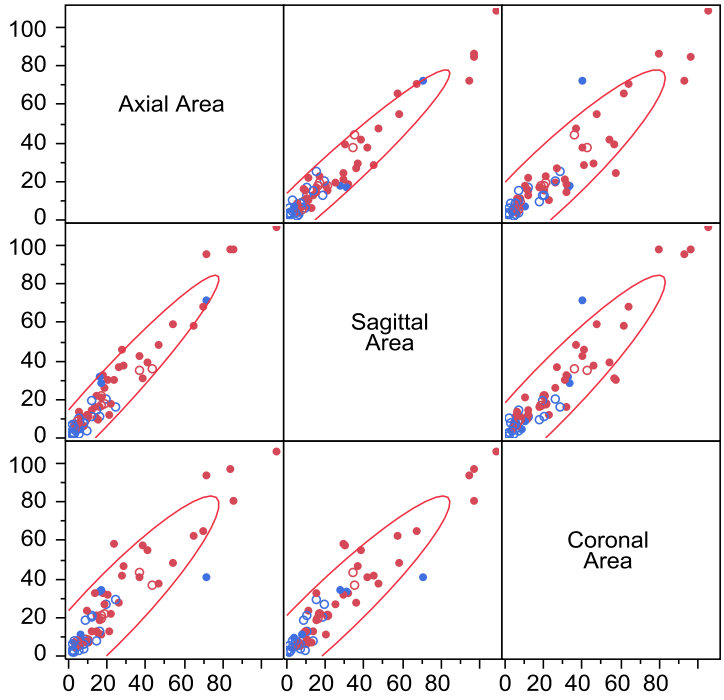

Figure 18: Correlation between the Areas

The correlation between the two raters is shown in Table 16.

Table 16: Correlation between Raters

Measurement	Correlation
Axial	
Length	0.80
Width	0.78
Area	0.83
Sagittal	
Length	0.82
Width	0.79
Area	0.87
Coronal	
Length	0.80
Width	0.85
Area	0.87

Table 17: Clinical Chart Data

Clinical Resident	Pt	Surgery Date	Tooth	Root	Sex	Age	Ethnicity	Obs Dehisc	Fenestr	Perf
JH	1	10/14/11	30	M	F	53	W	N	N	Y
JH	2	10/14/11	30	D	F	53	W	N	N	N
TA	3	6/8/12	4		M	64	W	N	Y	Y
PD	4	1/4/12	5		M	67	W	Y	N	Y
PD	5	2/1/12	9		M	31	W	N	N	Y
JH	6	2/17/12	24		F	77	W	Y	N	Y
JH	7	10/4/11	21		F	50	A	N	N	Y
TA	8	2/13/12	12	MB	M	37	H	N	N	Y
TA	9	2/13/12	12	DB	M	37	H	N	Y	Y
JC	10	1/9/12	19	M	F	16	W	N	N	Y
JC	11	1/9/12	19	D	F	16	W	N	N	N
PD	12	11/9/11	14	MB	M	65	W	N	N	Y
PD	13	11/9/11	14	DB	M	65	W	N	N	N
JC	14	11/2/11	3	MB	F	77	W	Y	N	N
JC	15	11/2/11	3	DB	F	77	W	N	N	N
JH	16	4/10/12	6		M	65	W	N	N	Y
TA	17	6/19/12	14	MB	M	38	W	N	Y	Y
TA	18	6/19/12	14	DB	M	38	W	N	Y	N
PD	19	9/14/11	19	M	M	74	W	N	Y	N
PD	20	9/14/11	19	D	M	74	W	N	N	N
JC	21	11/11/11	12		M	85	W	N	N	Y
DH	22	8/24/12	4		F	40	W	N	N	N
TA	23	4/27/12	25		M	31	B	Y	N	Y
JC	24	4/13/12	8		F	46	W	N	N	Y
JC	25	4/13/12	9		F	46	W	N	N	Y
PD	26	5/11/12	8		F	64	W	N	N	Y
PD	27	5/7/12	21		M	69	H	N	N	N
JH	28	10/19/11	14	MB	M	62	W	N	N	N
JH	29	10/19/11	14	DB	M	62	W	N	N	N
PD	30	10/31/11	25		M	71	W	Y	N	Y
JH	31	9/14/11	7		M	67	W	Y	Y	Y
DH	32	8/27/12	7		F	55	W	N	Y	N
TA	33	3/21/12	12		M	63	W	N	Y	Y
TA	34	3/14/12	14	MB	F	50	A	N	N	Y
TA	35	3/14/12	14	DB	F	50	A	N	N	Y

Table 18: CBCT Analysis Data

Eval	Pt	Scan Date	Read Date	T#	Rt	Ax Perf	L	W	Sag Perf	L	W	Cor Perf	L	W
DH	1	9/23/11	8/23/12	30	M	N	4	2.8	U	4	2.8	N	3.2	3.2
DH	2	9/23/11	8/12/12	30	D	N	3.6	3	U	3.4	2.6	N	3.2	2.3
DH	3	5/4/12	8/12/12	4		Y	8.5	8.2	U	9	8.3	Y	8.7	7
DH	4	11/18/11	9/3/12	5		Y	5.6	5.5	U	6.7	5.7	Y	10.1	7.3
DH	5	1/4/12	8/12/12	9		Y	10.3	8.7	Y	9.6	9	U	9.4	8.7
DH	6	12/21/11	9/3/12	24		Y	6.8	5.4	Y	8.2	5.8	U	9.5	6.2
DH	7	9/7/11	8/23/12	21		Y	5.7	3.1	U	5.5	3.6	Y	7	5.8
DH	8	12/13/11	8/9/12	12	MB	Y	2.9	2.3	U	3.1	2.7	Y	2.7	2.3
DH	9	12/13/11	8/9/12	12	DB	Y	3.2	2.7	U	4.6	2.9	Y	3.3	2.1
DH	10	12/5/11	8/12/12	19	M	N	8.4	5.6	U	8.3	5.3	N	8.4	6.5
DH	11	12/5/11	9/3/12	19	D	N	3	1.8	U	2.5	1.8	N	2.4	2.1
DH	12	8/24/11	8/23/12	14	MB	Y	5.8	4.7	U	4.1	3.7	Y	5.1	3.1
DH	13	8/24/11	8/23/12	14	DB	N	3.5	2	U	4	3.1	N	2.4	1.5
DH	14	10/20/11	9/3/12	3	MB	Y	5.1	4.4	U	7.7	4.7	Y	8.4	5.1
DH	15	10/20/11	8/9/12	3	DB	Y	3.9	2.2	U	2.4	2	Y	3.9	3
DH	16	2/13/12	8/9/12	6		Y	11.9	11.6	Y	12.3	11.3	U	11.7	11.5
DH	17	5/18/12	9/3/12	14	MB	Y	9.7	9.4	U	11.8	10.3	Y	11	10.8
DH	18	5/18/12	8/12/12	14	DB	N	2.1	1.8	U	2.6	2.5	N	3.5	2.8
DH	19	7/15/11	9/3/12	19	M	N	5.9	3.6	U	3.8	3.5	N	6.1	2.6
DH	20	7/15/11	8/23/12	19	D	N	1.7	1.7	U	1.5	0.8	N	2.2	1.2
DH	21	10/18/11	9/3/12	12		Y	7.9	6	U	8.2	6.5	Y	10.3	5
DH	22	4/9/12	8/9/12	4		N	3.8	2.7	U	3.5	2.7	N	3.7	2
DH	23	3/30/12	8/12/12	25		Y	5.1	4.6	Y	8.3	5	U	8.2	5
DH	24	2/15/12	8/9/12	8		N	5.3	4.5	N	4.8	4.5	U	5.5	4.9
DH	25	2/15/12	8/12/12	9		Y	4.3	3.1	Y	4	3.5	U	3.2	2.5
DH	26	3/12/12	8/23/12	8		Y	4.1	3.8	Y	5.2	3.4	U	4.2	3.7
DH	27	2/6/12	8/23/12	21		N	4.1	3.8	U	4.6	3	N	6	4.4
DH	28	10/18/11	8/9/12	14	MB	N	7.4	4.3	U	4.5	4.5	N	6.8	5.4
DH	29	10/18/11	8/9/12	14	DB	N	2.2	1.5	U	3.3	2.6	N	2.7	2.7
DH	30	10/3/11	9/3/12	25		Y	5.2	5	Y	6.2	6.1	U	7.9	5.1
DH	31	8/3/11	8/23/12	7		Y	8.7	5.7	Y	10.8	3.6	U	12.4	5.9
DH	32	6/25/12	8/12/12	7		N	4.4	4.4	N	4.4	4	U	3.2	3.1
DH	33	1/26/12	8/12/12	12		Y	4.6	4.2	U	5.5	5	Y	5.8	4.6
DH	34	1/11/12	8/9/12	14	MB	Y	2.5	2.1	U	2.5	2.2	Y	2.5	2.3
DH	35	1/11/12	8/23/12	14	DB	Y	3.3	3.2	U	4.1	1.7	Y	3.1	2.7
DH	10	12/5/11	9/9/12	19	M	N	8.5	5.6	U	8.3	5.1	N	8	6.6
DH	17	5/18/12	9/9/12	14	MB	Y	9.5	9.3	U	11.6	10.5	Y	10.7	10.5
DH	25	2/15/12	9/9/12	9		Y	4.2	3.2	Y	3.9	3.6	U	3.2	2.6
DH	29	10/18/11	9/9/12	14	DB	N	2.2	1.7	U	2.9	2.6	N	2.6	2.5
DH	34	1/11/12	9/9/12	14	MB	Y	3.1	2.4	U	3.1	2.3	Y	2.6	2.3
SR	1	9/23/11	9/21/12	30	M	N	2.9	2.1	U	3.3	3.1	N	3.3	2.8
SR	2	9/23/11	9/19/12	30	D	N	3.8	3.2	U	2.9	1.4	N	3.1	2.9
SR	3	5/4/12	9/19/12	4		Y	9	6.7	U	9	6.8	Y	7.3	6.5
SR	4	11/18/11	9/24/12	5		Y	5.1	4.3	U	5.5	4.7	Y	5.3	2.5
SR	5	1/4/12	9/19/12	9		Y	10.5	7.9	Y	9.5	7.8	U	10.4	7.6

SR	6	12/21/11	9/24/12	24		Y	6.3	5.6	Y	8	7.3	U	9	5.8
SR	7	9/7/11	9/21/12	21		Y	4.5	2.8	U	5.1	2.8	Y	6	5
SR	8	12/13/11	9/7/12	12	MB	Y	2.3	1.9	U	3.7	2.3	Y	2.9	2.8
SR	9	12/13/11	9/7/12	12	DB	N	5.3	4.1	U	6.2	4.4	N	6.1	4.3
SR	10	12/5/11	9/19/12	19	M	N	8.6	6.5	U	7.5	6	N	7.5	6.2
SR	11	12/5/11	9/24/12	19	D	N	2.5	1.8	U	1.7	1.1	N	2	1.3
SR	12	8/24/11	9/24/12	14	MB	Y	4.8	4.1	U	4.1	2.8	Y	4.9	3.1
SR	13	8/24/11	9/24/12	14	DB	N	2.7	2.6	U	2.3	1	N	3.2	1.9
SR	14	10/20/11	9/24/12	3	MB	Y	4.9	4.4	U	7.5	5.3	Y	7.6	5.5
SR	15	10/20/11	9/7/12	3	DB	Y	3.8	2.3	U	3.6	2.8	Y	4.3	3.3
SR	16	2/13/12	9/7/12	6		Y	11.8	9.1	Y	12.2	10.2	U	12.4	9.9
SR	17	5/18/12	9/24/12	14	MB	Y	10.8	10.1	U	12.3	10.1	Y	10.3	9.9
SR	18	5/18/12	9/19/12	14	DB	Y	9.8	9.3	U	10	9.1	Y	8	6.5
SR	19	7/15/11	9/24/12	19	M	N	2.5	1.4	U	3.2	1.1	N	2.8	1.1
SR	20	7/15/11	9/21/12	19	D	N	1.8	1.7	U	1.5	1.3	N	1.7	1.2
SR	21	10/18/11	9/24/12	12		Y	7.9	6.6	U	7.9	6.2	Y	11.2	6.2
SR	22	4/9/12	9/7/12	4		N	3.5	3.1	U	3.4	2.7	N	3.5	1.1
SR	23	3/30/12	9/19/12	25		N	5	4.5	N	5.1	4.2	U	5.5	4.4
SR	24	2/15/12	9/7/12	8		Y	6	4.7	Y	4.9	4.5	U	5.3	5.2
SR	25	2/15/12	9/19/12	9		Y	3.7	3.6	Y	3.8	3.6	U	3.5	3
SR	26	3/12/12	9/21/12	8		Y	4.7	4	Y	3.8	3.3	U	4.3	3.7
SR	27	2/6/12	9/21/12	21		N	4	2.8	U	4.2	2.7	N	5.4	4.3
SR	28	10/18/11	9/7/12	14	MB	N	6.8	3.7	U	5.1	5	N	6.8	4.9
SR	29	10/18/11	9/7/12	14	DB	N	1.6	1.5	U	2.9	2.6	N	2.7	2.2
SR	30	10/3/11	9/24/12	25		Y	5.4	4.5	Y	5.9	5.6	U	6.9	4.9
SR	31	8/3/11	9/21/12	7		Y	6.3	5.4	Y	7.2	6.5	U	6	5.8
SR	32	6/25/12	9/19/12	7		N	4.5	3.6	N	5.1	4.8	U	5.1	4.9
SR	33	1/26/12	9/19/12	12		Y	4.8	4.4	U	4.7	4.3	Y	5.3	4.3
SR	34	1/11/12	9/7/12	14	MB	Y	2.7	2.6	U	3.5	2.7	Y	2.5	2.4
SR	35	1/11/12	9/28/12	14	DB	Y	3.1	2.5	U	4.9	3.4	Y	3.1	2.6
SR	10	12/5/11	2/15/13	19	M	N	8.4	6	U	7.6	5.2	N	7.6	5.8
SR	17	5/18/12	2/15/13	14	MB	Y	11	10.3	U	10.2	9.8	Y	10.3	9.5
SR	25	2/15/12	2/15/13	9		Y	3.5	2.9	Y	3.6	3.4	U	3.3	2.9
SR	29	10/18/11	2/15/13	14	DB	N	2	1.7	U	3.2	2.7	N	2.8	1.9
SR	34	1/11/12	2/15/13	14	MB	Y	2.5	1.9	N	3.2	2.7	Y	2.5	2

Vita

Dr. Dan-Linh Ha was born on June 24, 1982, in Vancouver, British Columbia, Canada, and is a Canadian citizen. Dr. Ha received her Bachelor of Science in Biology from the University of British Columbia in 2005 and subsequently worked as a dental assistant and receptionist for Dr. Carol L. Tsuyuki for one year. She received her Doctor of Dental Surgery in 2010 and Certificate in Hospital Dentistry in 2011 from Indiana University. Dr. Ha then enrolled in the Advanced Specialty Program in Endodontics at Virginia Commonwealth University, School of Dentistry. Dr. Ha is a member of the CAE, AAE and ADA and will enter private practice in Victoria, British Columbia. She will graduate from Virginia Commonwealth University with a Master of Science in Dentistry and a Certificate in Endodontics.